ELSEVIER

Ab initio molecular treatment for charge transfer by S³⁺ ion on hydrogen

M. Łabuda [a,b], Y.S. Tergiman [a], M.-C. Bacchus-Montabonel [a,*], J.E. Sienkiewicz [b]

[a] *Laboratoire de Spectrométrie Ionique et Moléculaire, UMR 5579, CNRS et Université Lyon I, 43 Bd. du 11 Novembre 1918, F-69622 Villeurbanne Cedex, France*
[b] *Department of Theoretical Physics and Mathematical Methods, Gdańsk University of Technology, ul. Narutowicza 11/12, Pl-80-952 Gdańsk, Poland*

Abstract

Potential energy curves and coupling matrix elements of the one-electron capture by S³⁺ ions in collision with atomic hydrogen have been determined at the multi-reference configuration interaction level of theory. These calculations show evidence of an untabulated $S^{2+}(3s^23p3d)^3F^0$ capture level, already pointed out by translational energy spectroscopy experiments, which is necessary to explain the charge transfer mechanism. Calculated cross-sections are in good agreement with the experimental measurements.
© 2004 Elsevier B.V. All rights reserved.

1. Introduction

Charge transfer processes involving low-energy multiply charged ions in collision with atomic or molecular targets are determinant in laboratory and astrophysical plasmas. In such processes, an electron is generally captured in an excited state of the ion, followed by line emission. Line intensities provide important information on the electron temperature, density and spatial distributions in the emitting region of the plasma. An accurate understanding of the emergent spectra of emission-line astrophysical objects requires a detailed modeling of the atomic and molecular processes affecting conditions in the gas, as collisional excitation, photodissociation, but also charge transfer processes which appear to be essential for the determination of the ion abundances and ionization balance of the plasmas [1–3].

Sulphur ions play an important role in the reactions occurring in the interstellar medium [4,5], but charge transfer processes involving such ions remain up-to-now scarcely investigated theoretically [6–8], as well as experimentally [9,10]. From the experimental point of view, state-selective electron capture by S³⁺ ions in H, H₂ and He at impact energies within the range 2.4–9.0 keV have been studied by translational energy spectroscopy technique [10]. These experiments show evidence of an untabulated S^{2+} triplet state, identified as the $S^{2+}(3s^23p3d)^3F^0$ level, lying 15.03 eV above the S^{2+} ground state, which appear to be the dominant capture channel in the S³⁺ + H collision system over the entire range of impact energies investigated. No theoretical studies have been performed yet on this process in order to support the experimental conclusions, and the multichannel Landau–Zener approach fails to reproduce the experimental spectra, in particular it largely underestimates the capture on peak A relied to the $S^{2+}(^3F^0)$ level. We have thus undertaken a theoretical study of the $S^{3+}(3s^23p)$ + H reaction involving an accurate ab initio molecular calculation of the potential energy curves and couplings for the molecular

---
* Corresponding author. Fax: +33 0 4 72 43 15 07.
E-mail address: bacchus@lasim.univ-lyon1.fr (M.-C. Bacchus-Montabonel).

states involved in the process followed by a semiclassical dynamics in the 2–8 keV laboratory energy range where experimental data are available [10]. The calculation has been performed for the ground state S^{3+} + H entry channel only; the metastable ion $S^{3+}(3s3p^2)^4P$ evidenced in the ion beam, has not been taken into account in this study.

2. Potential energy curve calculations

The potential energy curves have been carried out using the MOLPRO suite of ab initio programs [11] at the state average CASSCF–MRCI level of theory. The active space includes the $n = 3$ and $n = 4(sp)$ orbitals for the sulphur element, and the 1s orbital for hydrogen. A pseudopotential has been used to take account of the core electrons of the sulphur atom. Different tests have been performed for the choice of this pseudopotential and the basis set of atomic orbitals. The ECP10sdf 10 core-electron relativistic pseudopotential has been used for sulphur [12] with the correlation-consistent aug-cc-pVQZ basis sets of Dunning [13] while the aug-cc-pV6Z basis has been chosen for hydrogen. Such a basis set shows a quite good agreement with experiment [14] for the atomic energy levels with a discrepancy in the range 0.01–0.14 eV (Table 1). The spin-orbit effects may be neglected in the collision energy range of interest so triplet and singlet manifolds can be considered separately.

From the atomic energy level data [14], it appears clearly that the $S^{2+}(3s^2 3p3d)^3P^0$ electron capture level cannot account for the present charge transfer mechanism. Effectively, the asymptotic energy difference between the entry channel $^{1,3}\Pi$, $^{1,3}\Sigma^+ \{S^{3+}(3s^2 3p)^2P^0 + H(1s)^2S\}$ and the capture levels correlated to the $\{S^{2+}(3s^2 3p3d)^3P^0 + H^{+1}S\}$ configuration is shown in tables [14] to be equal to 3.65 eV (0.13419 a.u.), quite different from the energy defect of 6.2 eV observed experimentally for peak A. From the asymptotical repulsion term, this energy difference would lead to a long range interaction with an avoided crossing around $R = 15$ a.u. which could hardly explain an important population of the corresponding capture channel. It seems thus likely, as proposed by Wilson et al. [10], to consider the possibility of an untabulated capture level $S^{2+}(3s^2 3p3d)^3F^0$, accessible from the entry channel $^{1,3}\Pi$, $^{1,3}\Sigma^+ \{S^{3+}(3s^2 3p)^2P^0 + H(1s)^2S\}$. The collisional

Table 1
Comparison of atomic energy levels with experiment [14] (in eV)

	MRCI calculation	Experiment
$S^{3+}(3s^2 3p)^2P^0$	35.11	34.98
$S^{2+}(3s3p^3)^3S^0 + H^+$		17.05
$S^{2+}(3s3p^3)^3P^0 + H^+$	12.31	12.17
$S^{2+}(3s3p^3)^3D^0 + H^+$	10.34	10.35
$S^{2+}(3s^2 3p^2)^3P + H^+$	0.0	0.0

system appears thus relatively complex, and a great number of states have to be taken into account in both the triplet and singlet manifold including one-electron capture processes as well as reactions of capture and excitation of the core electron 3s:

$S^{3+}(3s^2 3p)^2P^0 + H(1s)^2S$	$^3\Pi, {}^3\Sigma^+$	$^1\Pi, {}^1\Sigma^+$	entry channel
$S^{2+}(3s3p^3)^1P^0 + H^{+1}S$		$^1\Pi, {}^1\Sigma^+$	
$S^{2+}(3s3p^3)^3S^0 + H^{+1}S$	$^3\Sigma^-$		
$S^{2+}(3s3p3d)^3F^0 + H^{+1}S$	$^3\Phi, {}^3\Pi, {}^3\Delta, {}^3\Sigma^+$		
$S^{2+}(3s3p^3)^1D^0 + H^{+1}S$		$^1\Pi, {}^1\Delta, {}^1\Sigma^-$	
$S^{2+}(3s3p^3)^3P^0 + H^{+1}S$	$^3\Pi, {}^3\Sigma^+$		
$S^{2+}(3s3p^3)^3D^0 + H^{+1}S$	$^3\Pi, {}^3\Delta, {}^3\Sigma^-$		
$S^{2+}(3s^2 3p^2)^1S + H^{+1}S$		$^1\Sigma^+$	
$S^{2+}(3s^2 3p^2)^1D + H^{+1}S$		$^1\Pi, {}^1\Delta, {}^1\Sigma^+$	
$S^{2+}(3s^2 3p^2)^3P + H^{+1}S$	$^3\Pi, {}^3\Sigma^-$		

The potential energy curves correlated to the $S^{3+}(3s^2 3p)^2P^0$ + H entry channel are displayed in Fig. 1a,b for the triplet manifold, the corresponding results for the singlet manifold are available on request. The Σ^- levels are not correlated to the entry channel and have not been calculated.

According to the statistical weight, the triplet manifold accounts for 3/4 of the population of the ground state entry channel, against 1/4 for the singlet manifold, and appears thus to be preponderant in the charge transfer mechanism. Effectively, the $^1\Sigma^+$ states appear almost inactive in the charge transfer mechanism. An efficient avoided crossing may however be considered near $R = 7$ a.u. between the $^1\Pi$ entry channel and the $^1\Pi$ $\{S^{2+}(3s3p^3)^1D^0 + H^{+1}S\}$ level, it corresponds to an energy defect of 8.2 eV and may contribute to the experimental peak B. The triplet potential energy curves show several avoided crossings which may play a quite important role. Two short range avoided crossings are observed with the $^3\Pi$, $^3\Sigma^+$ levels corresponding to the $\{S^{2+}(3s3p^3)$ $^3P^0 + H^{+1}S\}$ configuration, around $R = 6$ a.u.; they are associated to an energy defect of 9.19 eV and may contribute to the experimental peak B. An other interaction appears with the $^3\Pi\{S^{2+}(3s3p^3)$ $^3D^0 + H^{+1}S\}$ level, around $R = 5$ a.u., which may contribute to peak C, with an energy defect of 11.16 eV. But the most important feature appears for the state quoted 4 in Fig. 1a,b which exhibits an avoided crossing around $R = 9.7$ a.u., corresponding to an energy defect of 5.6 eV, with the entry channel in both $^3\Sigma^+$ and $^3\Pi$ symmetries. This channel is associated simultaneously to state symmetry $^3\Sigma^+$, $^3\Delta$, $^3\Pi$, and $^3\Phi$ and may thus be attributed without any ambiguity to the $\{S^{2+}(3s3p3d)^3F^0 + H^{+1}S\}$ configuration, confirming the experimental deduction of Wilson et al. [10]. The energy defect appears however slightly lower than evidenced for the experimental peak A. From our ab initio MRCI calculations, the $S^{2+}(^3F^0)$ capture level
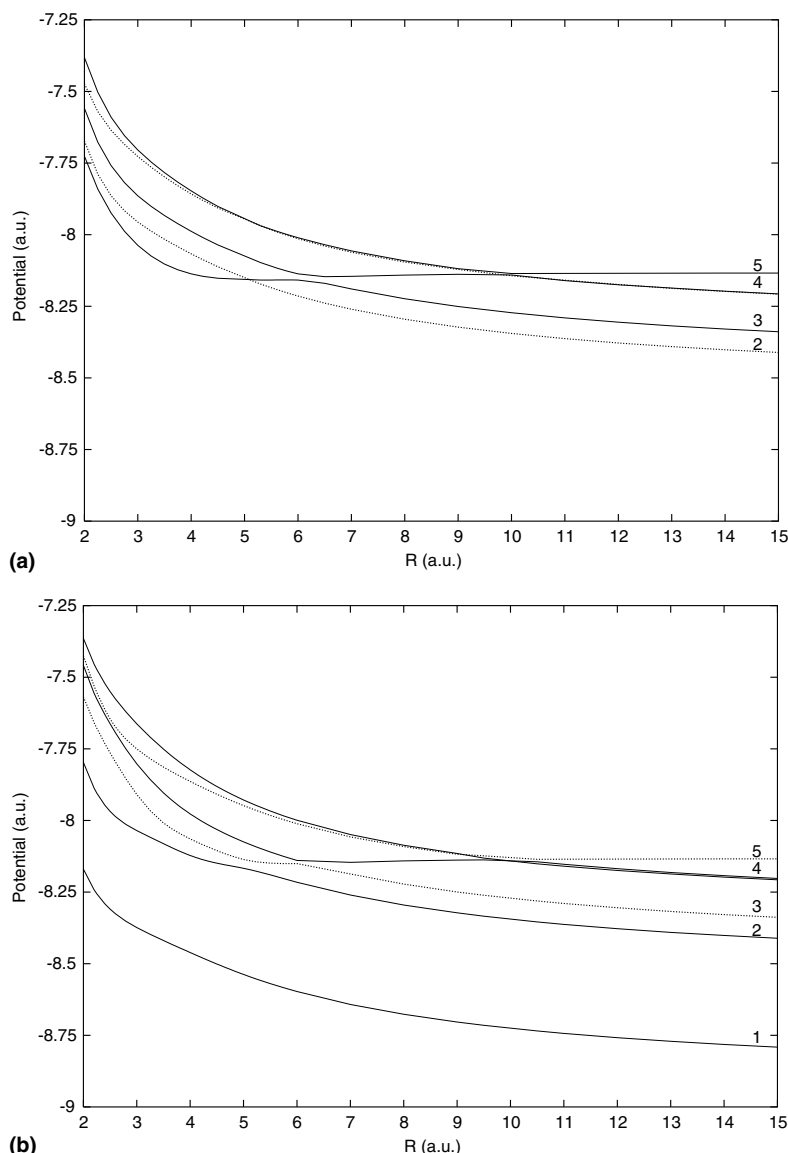
Fig. 1. (a): Adiabatic potential energy curves of the $^3\Sigma^+$ and $^3\Delta$ states of the $S^{3+}(3s^23p)$ + H collisional system. —, $^3\Sigma^+$ states; ----, $^3\Delta$ states. (2) $^3\Delta$ state corresponding to $\{S^{2+}(3s3p^3)^3D^0 + H^{+1}S\}$. (3) $^3\Sigma^+$ state corresponding to $\{S^{2+}(3s3p^3)^3P^0 + H^{+1}S\}$. (4) $^3\Sigma^+$ and $^3\Delta$ states corresponding to $\{S^{2+}(3s^23p3d)^3F^0 + H^{+1}S\}$. (5) $^3\Sigma^+$ state corresponding to $\{S^{3+}(3s^23p)^2P^0 + H(1s)^2S\}$ entry channel. (b): Adiabatic potential energy curves of the $^3\Pi$ and $^3\Phi$ states of the $S^{3+}(3s^23p)$ + H collisional system. —, $^3\Pi$ states; ----, $^3\Phi$ state. (1) $^3\Pi$ state corresponding to $\{S^{2+}(3s^23p^2)^3P + H^{+1}S\}$. (2) $^3\Pi$ state corresponding to $\{S^{2+}(3s3p^3)^3D^0 + H^{+1}S\}$. (3) $^3\Pi$ state corresponding to $\{S^{2+}(3s3p^3)^3$ $P^0 + H^{+1}S\}$. (4) $^3\Pi$ and $^3\Phi$ states corresponding to $\{S^{2+}(3s^23p3d)^3F^0 + H^{+1}S\}$. (5) $^3\Pi$ state corresponding to $\{S^{3+}(3s^23p)^2P^0 + H(1s)^2S\}$ entry channel.

appears at an energy of 15.8 eV above the $S^{2+}(3s^23p^2)^3P$ ground state, a somewhat higher value than the experimental one, although the set of molecular calculations appears to be globally in good accordance with the tabulated energies as shown in Table 2.

3. Radial and rotational couplings

The radial coupling matrix elements between all pairs of states of the same symmetry have been calculated by means of the finite difference technique:

$$g_{KL}(R) = \langle \psi_K \mid \partial/\partial R \mid \psi_L \rangle = \lim_{\Delta \to 0} \frac{1}{\Delta} \langle \psi_K(R) \mid \psi_L(R + \Delta) \rangle,$$

with the parameter $\Delta = 0.0012$ a.u. as previously tested and using the three-point numerical differentiation method for reasons of numerical accuracy. The sulphur nucleus has been chosen as origin of electronic coordinates. The main matrix elements are displayed in Fig. 2a,b for the triplet manifold. They present the same features as exhibited by the potential energy curves. The $^3\Sigma^+$ states show two peaks, one around $R = 6$ a.u. corresponding to the avoided crossing between the entry channel and the $^3\Sigma^+\{S^{2+}(3s3p^3)^3P^0 + H^{+1}S\}$ capture level associated to the experimental peak B, and a sharper

Table 2
Comparison with experiment [14] for asymptotic energy levels (in a.u.)

	MRCI calculation	Experiment
$S^{3+}(3s^23p)^2P^0 + H(1s)^2S$	0.0	0.0
$S^{2+}(3s3p^3)^3S^0 + H^+$		−0.1572
$S^{2+}(3s3p^3)^1P^0 + H^+$	−0.1477	−0.1628
$S^{2+}(3s3p3d)^3F^0 + H^+$	−0.2063	−0.2313[a]
$S^{2+}(3s3p^3)^1D^0 + H^+$	−0.3019	−0.3117
$S^{2+}(3s3p^3)^3P^0 + H^+$	−0.3379	−0.3363
$S^{2+}(3s3p^3)^3D^0 + H^+$	−0.4105	−0.4032
$S^{2+}(3s^23p^2)^1S + H^+$	−0.6601	−0.6625
$S^{2+}(3s^23p^2)^1D + H^+$	−0.7371	−0.7347
$S^{2+}(3s^23p^2)^3P + H^+$	−0.7905	−0.7837

[a] Ref. [10]

one, around $R = 9.7$ a.u., in correspondence with the strong avoided crossing between the entry channel and the $^3\Sigma^+\{S^{2+}(3s^23p3d)^3F^0 + H^{+1}S\}$ excited one-electron capture level. This radial coupling matrix element reaches 2.75 a.u. and is clearly the most important one for the charge transfer process, associated to the experimental peak A. Radial coupling between $^3\Delta$ states remain small for all internuclear distances. The $^3\Pi$ levels show also such a sharp peak for the radial coupling corresponding to the avoided crossing with the $^3\Pi\{S^{2+}(3s^23p3d)^3F^0 + H^{+1}S\}$ capture channel. It reaches even 3.5 a.u. and is markedly higher that the other radial coupling matrix elements. The coupling
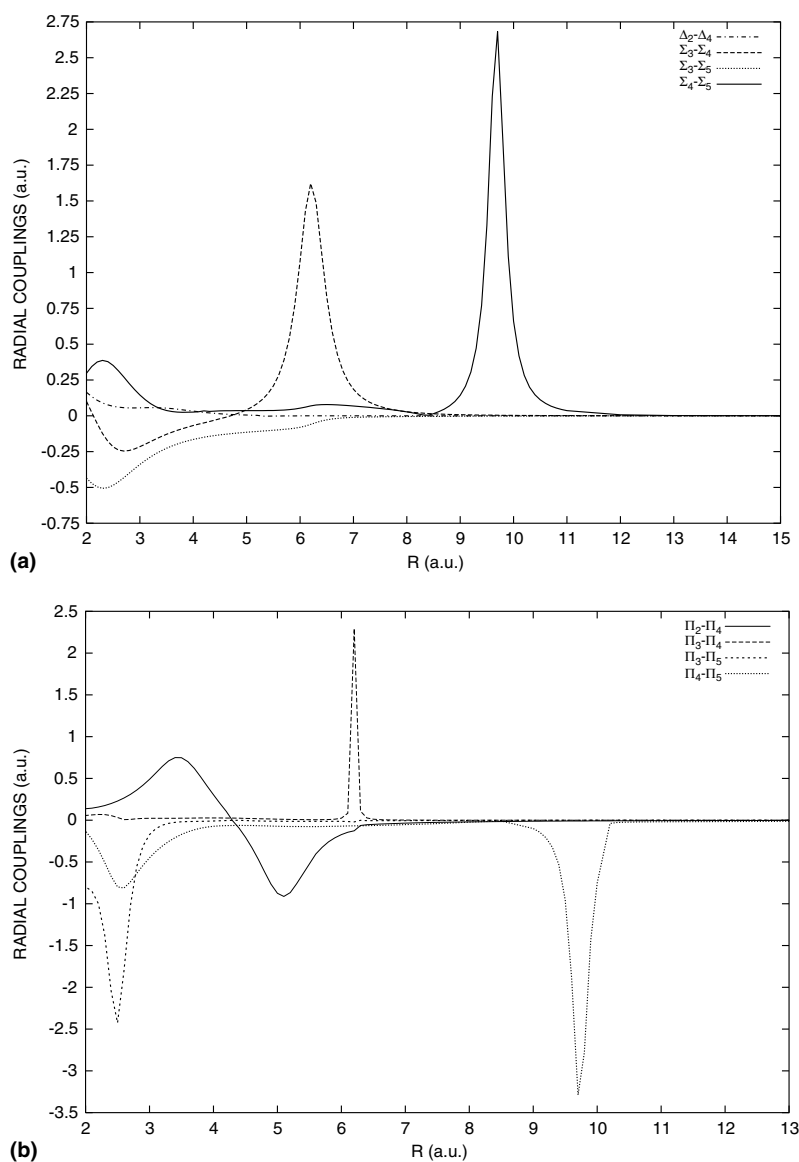

Fig. 2. (a) Radial coupling matrix elements between $^3\Sigma^+$ and $^3\Delta$ states of the $S^{3+}(3s^23p) + H$ collisional system (see labels in Fig. 1a). (b) Radial coupling matrix elements between $^3\Pi$ states of the $S^{3+}(3s^23p) + H$ collisional system (see labels in Fig. 1b).

associated with the avoided crossing between the $^3\Pi$ entry channel and the $^3\Pi\{S^{2+}(3s3p^3)^3P^0 + H^{+1}S\}$ level presents a peak, 2.5 a.u. high, around $R = 6$ a.u. and the interaction with the $^3\Pi\{S^{2+}(3s3p^3)^3D^0 + H^{+1}S\}$ capture channel shows a smooth variation of the radial coupling matrix element with a hump around $R = 5$ a.u.

The rotational matrix elements $\langle\psi_K|iL_y|\psi_L\rangle$ between states of angular moment $\Delta\Lambda = \pm 1$ have been calculated directly from the quadrupole moment tensor. The coupling matrix elements for the triplet manifold are displayed in Fig. 3. Rotational couplings between Σ–Π and Π–Δ are zero at long range for states corresponding to different configurations, as shown for example for the coupling between $^3\Sigma^+\{S^{3+}(3s3p^3)^3P^0 + H^{+1}S\}$ and $^3\Pi$ $\{S^{2+}(3s3p^3)^3D^0 + H^{+1}S\}$ levels. The couplings corresponding to the same configuration reach the asymptotical value 1.0 a.u., as shown for the $^3\Sigma^+$–$^3\Pi$ couplings corresponding to the $\{S^{3+}(3s^23p)^2P^0 + H(1s)^2S\}$ and the $\{S^{2+}(3s3p^3)^3P + H^{+1}S\}$ configurations, as well as to the $^3\Pi$–$^3\Delta$ rotational couplings associated to the $\{S^{2+}(3s3p^3)^3D^0 + H^{+1}S\}$ configuration. For the $\{S^{2+}(3s^23p3d)^3F^0 + H^{+1}S\}$ capture channel, both $^3\Sigma^+$ and $^3\Delta$ states contribute to the rotational coupling with the $^3\Pi$ level, giving a double value for the matrix element. In correspondence with the crossing between this $S^{2+}(3s^23p3d)^3F^0$ capture level and the entry channel, an abrupt decrease may be observed for this rotational coupling to reach the value around 1.0 a.u. corresponding to the $^3\Sigma_5$–$^3\Pi_5$ coupling of the entry channel, and inversely.

4. Collision dynamics

The collision dynamics has been treated from these molecular data by a semiclassical approach using the EI-ΚΟΝΧS program [15] based on an efficient propagation method in the 2–8 keV laboratory energy range, in order to be compared to the experimental data. Both radial and rotational coupling matrix elements were taken into account, as well as translational effects using common translation factors as proposed by Errea et al. [16]. The sulphur nucleus has been taken as origin of the electronic coordinates. The cross-sections corresponding to the different exit channels have been calculated with respect to the statistical weights 1/4 and 3/4 for, respectively, the singlet and triplet manifold, and taking account of the 1/3 and 2/3 statistical weight for, respectively, the Σ and Π entry channels. The results are presented in Table 3 and appear to be in good agreement with the experimental data. Effectively, the $S^{2+}(3s^23p3d)^3F^0$ capture channel attributed to peak A is clearly the dominant charge transfer channel, with a ratio σ_A/σ_B for the partial cross-sections between peak A and peak B corresponding mainly to the $S^{2+}(3s3p^3)^3P^0$ capture level around 1.3 as observed on

Fig. 3. Rotational coupling matrix elements between $^3\Sigma^+$–$^3\Pi$ and $^3\Pi$–$^3\Delta$ states of the $S^{3+}(3s^2\ 3p) + H$ collisional system (see labels in Fig. 1a,b). ······, $\Sigma_4 + \Delta_4/\Pi_4$; --·--, Σ_5/Π_5; -----, Σ_3/Π_3; · · · ·, Δ_2/Π_2; full line, Σ_3/Π_2

Table 3
Partial cross-sections on the different exit channels in the $S^{3+}(3s^23p)^2P^0 + H$ process (in 10^{-16} cm^2)

E_{lab} keV	$S^{2+}(3s3p^3)^1P^0$	$S^{2+}(3s3p3d)^3F^0$, peak A	$S^{2+}(3s3p^3)^1D^0$, peak B	$S^{2+}(3s3p^3)^3P^0$, peak B	$S^{2+}(3s3p^3)^3D^0$, peak C	$S^{2+}(3s^23p^2)^3P$	σ_A/σ_B	σ_B/σ_C
2.002	0.06	17.63	0.02	9.49	6.40	0.0001	1.8	1.5
2.883	0.79	16.29	0.03	11.90	6.85	0.0004	1.3	1.7
3.924	0.63	14.57	0.05	12.19	8.08	0.0006	1.2	1.5
5.125	0.73	13.54	0.12	10.54	7.78	0.0016	1.3	1.3
6.487	0.73	13.08	0.23	9.52	7.87	0.0018	1.3	1.2
8.009	0.87	11.85	0.31	8.37	7.63	0.0036	1.3	1.1

the experimental spectra. Both peaks A and B are shown to decrease at higher energies. The partial cross-section on peak C corresponding to the $S^{2+}(3s3p^3)^3D^0$ exit channel is slightly underestimated and remains always lower than peak B, nevertheless it increases at higher energies and reaches the same order of magnitude as peak B as observed experimentally. The partial cross-sections on the $S^{2+}(3s3p^3)^1P^0$ channel increases also with energy but remains much lower. The cross-sections towards the $S^{2+}(3s^23p^2)^1S$ and $S^{2+}(3s^23p^2)^1D$ exit channels are almost zero for all collision energies, and the cross-sections on the $S^{2+}(3s^23p^2)^3P$ capture channel cross-sections on the $S^{2+}(3s^23p^2)^3P$ capture channel remain negligible.

5. Concluding remarks

This work provides accurate molecular data, potential energy curves as well as radial and rotational coupling matrix elements, for the $S^{3+}(3s^23p)^2P^0 + H(1s)^2S$ collisional system. Contrary to the previous Landau–Zener approach, a semiclassical collisional treatment taking account of radial and rotational couplings can reproduce the experimental data and gives a clear insight into the charge transfer mechanism. This study provides a precise attribution of the experimental spectra, and evidences in particular the existence of the

$\{S^{2+}(3s^23p3d)^3F^0 + H^{+1}S\}$ capture channel associated to the dominant experimental peak A already pointed out by translational energy spectroscopy [10].

References

[1] D. Péquignot, Astron. Astrophys. 81 (1980) 356.
[2] G.A. Shields, A. Dalgarno, A. Sternberg, Phys. Rev. A 28 (1983) 2137.
[3] J.B. Kingdon, G.J. Ferland, Astrophys. J. 516 (1999) L107.
[4] D. Péquignot, S.M.V. Aldrovandi, G. Stasinska, Astron. Astrophys. 63 (1978) 313.
[5] R. McCray, C. Wright, S. Hatchett, Astrophys. J. 211 (1977) L29.
[6] M.C. Bacchus-Montabonel, Chem. Phys. 228 (1998) 181.
[7] K. Amezian, M.C. Bacchus-Montabonel, Chem. Phys. Lett. 199 (1992) 487.
[8] S.E. Butler, A. Dalgarno, Astrophys. J. 241 (1980) 838.
[9] A. Al-Mulhem, I. Nasser, Phys. Rev. A 46 (1992) 2945.
[10] S.M. Wilson, T.K. McLaughlin, R.W. McCullough, H.B. Gilbody, J. Phys. B 23 (1990) 1315.
[11] H.-J. Werner et al., Molpro code (version 2002.1).
[12] A. Nicklass, M. Dolg, H. Stoll, H. Preuss, J. Chem. Phys. 102 (1995) 8942.
[13] D.E. Woon, T.H. Dunning Jr., J. Chem. Phys. 98 (1993) 1358.
[14] S. Bashkin, J.O. Stoner Jr., Atomic Energy Levels and Grotrian Diagrams, North-Holland, Amsterdam, 1978.
[15] R.J. Allan, C. Courbin, P. Salas, P. Wahnon, J. Phys. B 23 (1990) L461.
[16] L.F. Errea, L. Mendez, A. Riera, J. Phys. B 15 (1982) 101.